Analysis of Crack Phenomenon for Injection-Molded Screw Using Moldflow Simulation

Hyeyoung Shin,[1] Eun-Soo Park[2]

[1]*Kumho Petrochemical R&D Center, Hwaam-dong, Yuseong, Taejeon 305-348, Korea*
[2]*Youngchang Silicone Co., Ltd., Gasan-Dong, Kumchun-Gu, Seoul 153-803, Korea*

Received 13 January 2009; accepted 15 March 2009
DOI 10.1002/app.30412
Published online 28 April 2009 in Wiley InterScience (www.interscience.wiley.com).

ABSTRACT: The screw for ice water filter machine was injection molded with acrylonitrile–butadiene–styrene (ABS)/polycarbonate (PC) [ABS/PC] alloy resin and its crack phenomenon after mechanical stress was analyzed by commercial Moldflow software. The cracked morphology and tensile properties of ABS/PC have been studied by scanning electron microscopy (SEM) and universal test machine (UTM). The injection pressure and the residual stress has been compared with two injection molding conditions as actual manufacturing and reduced injection flow rate. This analysis has found that residual stress is higher at actual manufacturing condition. SEM study reveals that in the micrographs taken on the surface of cracked sample ABS rubber domains tend to extremely align in the direction of mold flow. The combined data suggest that the majority of the crack comes from residual stress in final part originated from higher injection pressure during injection-molding process. © 2009 Wiley Periodicals, Inc. J Appl Polym Sci 113: 2702–2708, 2009

Key words: simulations; alloys; electron microscopy; shear stress; ABS/PC

INTRODUCTION

Acrylonitrile–butadiene–styrene (ABS) resins are among the most versatile thermoplastics in the styrenic polymers. The primary features and benefits of ABS resins are derived from the tree building blocks. Thermal stability and chemical resistance are derived from acrylonitrile, whereas butadiene provides impact resistance and toughness. Styrene imparts rigidity and processability to ABS. Therefore, they have practical toughness, high modulus, dimension stability, and good esthetics for a broad range of applications.[1–4] These characteristics make them highly suitable for uses in automotive small and large appliances, information technology equipment, building and construction, electronics, and molding components because of their processability and cost efficiency.[4] Recent developments resulted in polymer blends of ABS with polypropylene,[5,6] polycarbonate (PC),[7–10] poly(buthylene terephthalate),[11] and nylon6[12] to improve mechanical properties and productivity. ABS/PC blends have light weight, good durability, superior adhesion properties, and dimensional stability over wide temperature range. Furthermore, they can be easily processed on extrusion, injection and compression molding equipment.

Correspondence to: E.-S. Park (t2phage@hitel.net).

Journal of Applied Polymer Science, Vol. 113, 2702–2708 (2009)

Injection molding is the most commonly used manufacturing process for the fabrication of plastic parts.[13–15] A wide variety of products are manufactured using injection molding, which vary greatly in their size and complexity. The injection molding process requires the use of an injection molding machine, raw plastic material, and a mold. The plastic is melted in the injection molding machine and then injected into the mold, where it cools and solidifies into the final part. The most common injection molding faults are operating at an incorrect injection pressure. Too low an injection pressure will result in a sink marks, whereas too high a pressure will lead to flash and core shift being formed.

Moldflow simulation programs are able to analyze the smallest medical device to the largest car instrument panel quickly and to give practical solutions to complex injection molding problems. Benefits that have been identified from experienced users of analysis programmed are better part quality, reduced tooling lead time, optimum cycle times, and reduce rework and scrapping of materials.[13–16] In this study, the screw for ice water filter machine was injection-molded with ABS /PC alloy resin using actual manufacturing condition and its crack phenomenon after equipped in ice water filter machine was studied by scanning electron microscopy (SEM) and Moldflow simulation. To investigate the effect of processing temperature on crack phenomenon, the tensile properties of hot-pressed ABS/PC sheets at 225, 250, and 275°C were also measured.

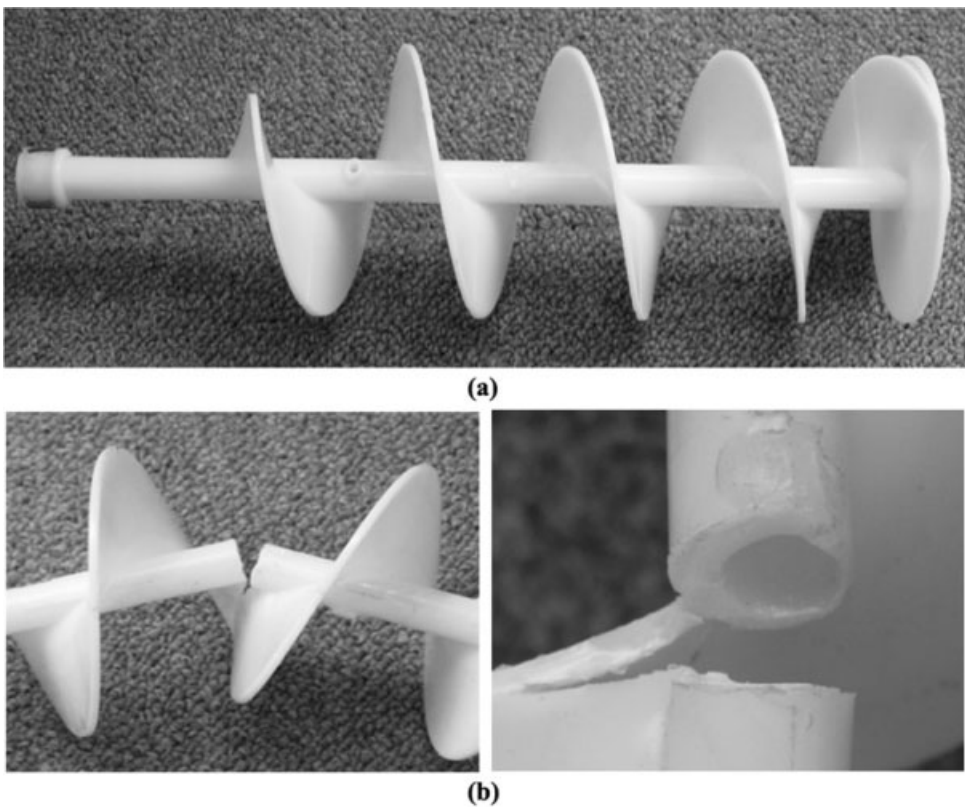

Figure 1 Images of the injection-molded screw and broken screw after equipped in ice water filter machine.

EXPERIMENTAL

Materials

ABS/PC alloy resin [HAC-8244 (density: 1.12 g/cm^3, melt index: 40 g/10 min under 21.6 kg loads at 230°C), Kumho Petrochemical Co., Seoul, Korea] was used as received. ABS/PC resin was predried in a convection oven for at least 12 h at 80°C to remove any moisture from the pellets before processing.

Injection molding of screw

Screw samples were injection molded at a speed of 70 rpm using a 350-ton injection-molding machine [IDE350EN (screw diameter: φ 60, maximum injection pressure: 1640 kg/cm^2, maximum injection rate: 362 cm^3/s), LG Cable Ltd., Anyang, Korea] equipped with a 1 : 3 compression ratio screw. The injection molding machine contains four different operational variables that is in the order of melt temperature (220, 225, 230, 235°C), injection pressure (60, 60, 55, 50, and 35 kg/cm^2), shot size (50, 30, 25, 20, and 10 mm), and injection speed (40, 50, 55, 30, and 25%).

Tensile test procedure

The ABS/PC alloy was subsequently hot pressed to samples of uniform thickness (around 0.6 mm) at 225, 250, or 275°C for 5 min under about 5 atm using a plate press and quickly immersed into water. The sheet thus formed was free from any distortion problems. Dumbbell specimens for mechanical tests were prepared in accordance with IEC60811-1-1 specification. The test specimens were preconditioned to 10% relative humidity and 20°C ± 1°C to standardize test conditions. Tensile properties of samples were determined with a universal test machine (UTM, Model DECMC00, Dawha test machine, Bucheon, Korea) at a crosshead speed of 250 mm/min. The mean value of at least five specimens of each sample was taken, although specimens that broke in an unusual manner were disregarded.

Morphology of cracked specimen

SEM observations of the specimens were performed on a JEOL JEM-1220 model (Tokyo, Japan). The JEOL JEM-1220 is a 120 kV transmission electron microscope (TEM) fitted with a LaB6 electron source. The sample surface was staining OsO_4 aqueous solution. The stained sample was microtomed using a diamond knife and the morphology was determined using an accelerating voltage of 30 kV.

Moldflow analysis

Moldflow (Moldflow 6.2, Moldflow Corporation, MA) analysis was conducted using a single cavity mold with direct sprue gating into the part. Several iterations were carried out to establish optimum

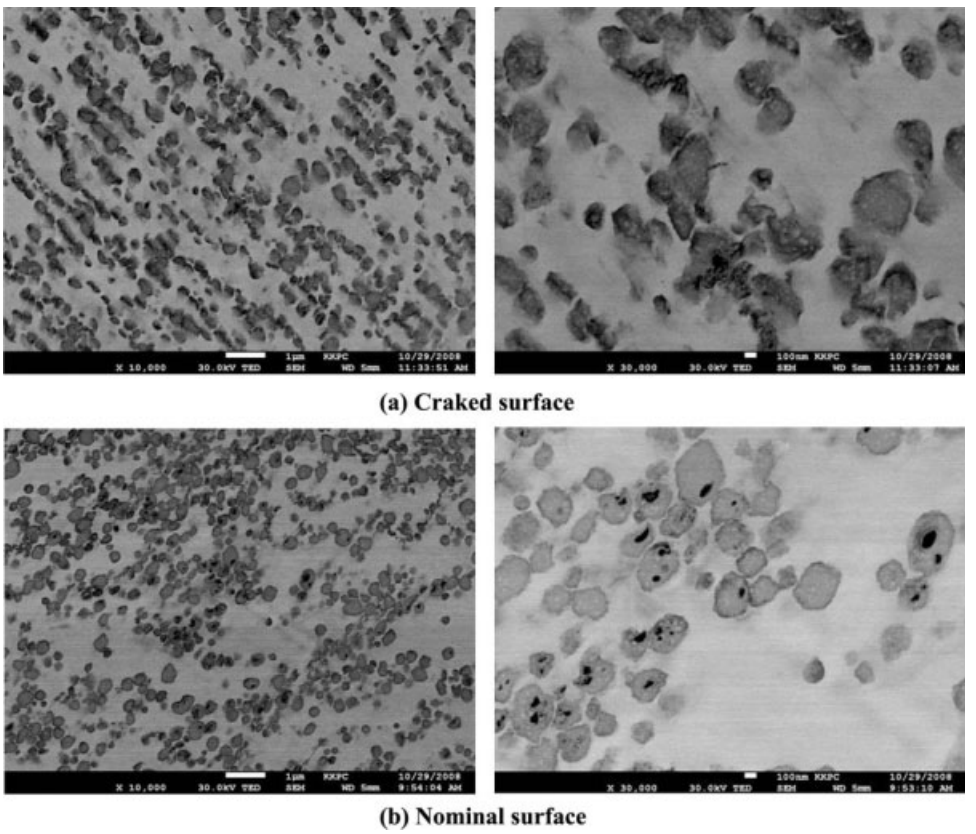

Figure 2 SEM micrographs of the microtomed surfaces of cracked and nominal injection-molded screw sample.

location of the sprue gate to achieve the most balanced flow into the cavity along with uniform pressure drop and flow front temperature. The 3D-CAD drawing of cover mold was exported to the FE software using STEP file format and modeled using MF/FLOW module of Moldflow. The surfaces of part were converted to a midsurface mesh via Moldflow Preprocessing.

RESULTS AND DISCUSSION

ABS/PC alloy resin was injection molded in a screw sample using actually used in factory. The image of the injection-molded screw and the broken screw after equipped in ice water filter machine was demonstrated in Figure 1. Crazing is the first stage of fracture in glassy polymers.[17] Under a sufficiently high stress, the fibrillar structure of craze breaks down and a true crack forms. When the crack reaches a critical size the material finally breaks [Fig. 1 (b)]. Core shifts [Fig. 1 (b)] are caused by an uneven distribution of the polymer melt flow around a core pin during filling and packing phases of the injection molding cycle. The deflection of the core causes wall thickness variation of the part. For high-precision parts, the core deflection can lead to rejects or a premature service life failure.

Figure 2 compares the microtomed and OsO_4 stained surfaces of the cracked and nominal injection-molded screw sample. An immiscible polymer blend system generally has a microstructure with the phase separation between components. The

TABLE I
Mechanical Properties of the ABS/PC Alloy Resin

Sample code	Tensile properties	
	Tensile strength (kg/mm^2)	Elongation at break (%)
ABS/PC-225	43 ± 4	135 ± 16
ABS/PC-250	42 ± 4	134 ± 22
ABS/PC-275	38 ± 7	27 ± 8

TABLE II
Processing Parameters of the Moldflow Simulation

Sample code	Unit	1st condition	2nd condition
Flow rate	cm^3/s	Multistep	50
Mold temperature	°C	50	50
Melt temperature	°C	Multistep	250
Filling/packing	–	Switch over at 98 vol %	Switch over at 98 vol %
Packing profile	–	80% of maximum pressure	80% of maximum pressure
Cooling times	s	45	30

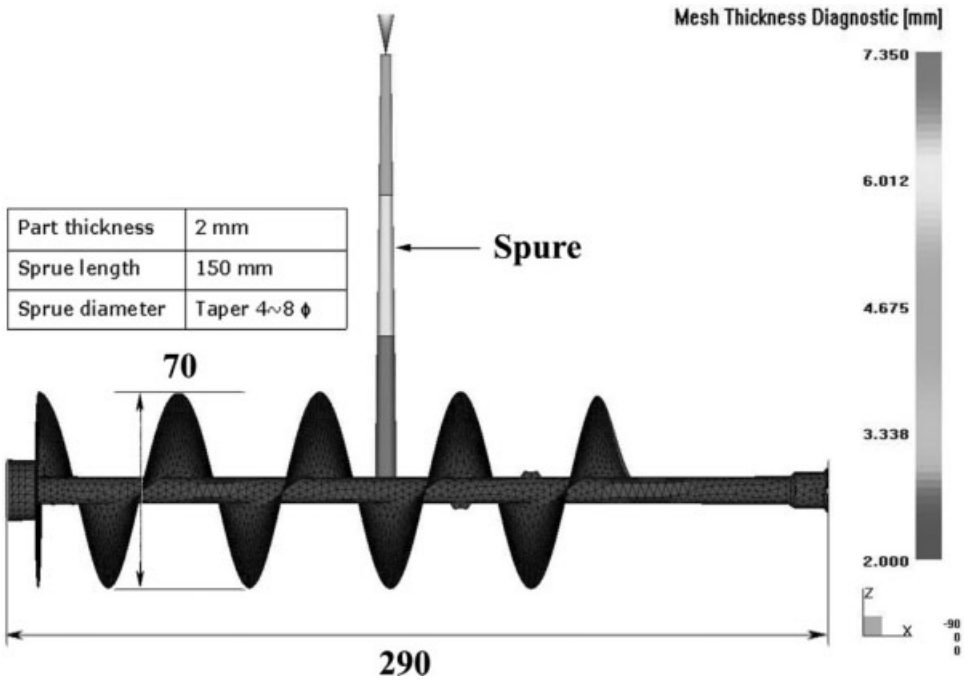

Figure 3 Single cavity mold with the direct sprue gating into screw part.

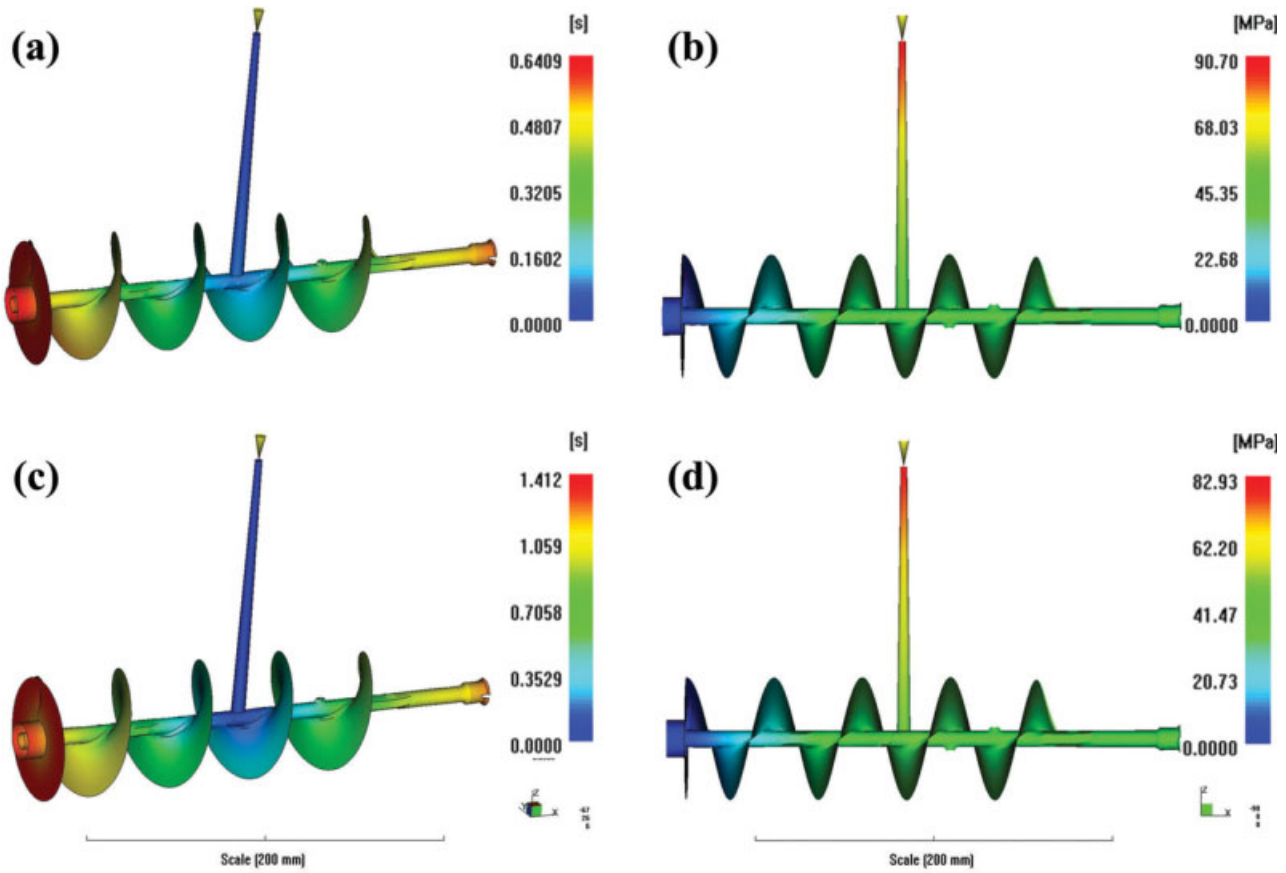

Figure 4 Results of the filling time [(a) 1st condition (c) 2nd condition] and injection pressure [(b) 1st condition (d) 2nd condition] analysis. [Color figure can be viewed in the online issue, which is available at www.interscience.wiley.com.]

TABLE III
Injection Pressure and Flow Rate Changes During Filling Stage

1st condition					2nd condition				
Time (s)	Volume (%)	Pressure (MPa)	Flow rate (cm^3/s)	Status	Time (s)	Volume (%)	Pressure (MPa)	Flow rate (cm^3/s)	Status
0.04	1.98	20.09	92.33	V	0.07	2.80	24.32	34.33	V
0.06	3.92	30.96	88.42	V	0.12	6.85	32.67	44.01	V
0.09	6.85	38.64	90.28	V	0.19	11.42	37.60	48.47	V
0.11	10.01	43.21	105.24	V	0.26	16.38	39.64	48.93	V
0.14	15.44	45.06	109.20	V	0.32	21.18	41.07	49.22	V
0.17	20.33	46.06	110.89	V	0.39	26.13	42.31	49.33	V
0.20	25.03	46.67	111.57	V	0.45	30.84	44.97	48.54	V
0.23	27.79	47.72	107.88	V	0.52	35.48	47.73	48.86	V
0.25	34.45	50.01	106.22	V	0.58	40.20	50.35	48.96	V
0.28	38.93	52.38	107.36	V	0.64	44.94	53.03	49.02	V
0.31	43.56	54.60	107.90	V	0.71	49.65	55.64	49.15	V
0.34	48.14	56.73	108.21	V	0.77	54.36	58.16	49.28	V
0.37	52.72	58.83	108.48	V	0.84	59.08	60.65	49.36	V
0.40	57.33	60.94	108.62	V	0.90	63.78	63.21	49.38	V
0.42	62.00	63.11	108.82	V	0.97	68.39	67.96	49.08	V
0.45	66.54	65.42	107.96	V	1.03	73.09	71.87	49.51	V
0.48	70.83	69.67	105.23	V	1.10	77.72	75.02	49.68	V
0.51	75.16	73.74	107.24	V	1.16	82.42	77.69	49.77	V
0.54	79.73	78.60	114.15	V	1.22	87.13	79.41	49.86	V
0.59	89.35	89.78	127.83	V	1.29	91.61	82.70	49.91	V
0.61	93.12	92.14	139.97	V	1.35	96.35	82.96	49.91	V
0.62	95.18	91.99	144.82	V	1.37	97.69	82.93	49.85	V/P
0.63	98.04	90.70	157.75	V/P	1.38	98.41	66.35	23.89	P
0.64	99.57	90.10	157.75	P	1.41	99.57	66.35	24.92	P
0.64	100.00	90.02	157.59	Filled	1.41	100.00	66.35	23.93	Filled

Status: V, velocity control; P, pressure control; V/P, velocity/pressure switchover.

major component in blends forms a continuous matrix, whereas the dispersed one assumes different forms such as droplet, rod, fibril, or lamella.[18,19] ABS/PC alloy actually consist of three components of PC, styrene–acrylonitrile (SAN), and polybutadiene (PB). PC was the continuous phase in alloy resin and ABS was dispersed in the PC matrix. ABS domains consisted of SAN matrix filled with rubber particles. In the SEM micrographs, the dark domains represents the PB phase in the ABS, whereas the light region represents SAN matrix.

In a rubber-toughened polymer, the function of the rubber particles is not only to initiate crazes but also to prevent, or last delay, the formation of crack of critical length. In the micrographs taken on the surface of cracked sample, ABS rubber domains tend to align in the direction of mold flow and they are usually parallel to the stretching polymer chains [Fig. 2 (a)]. Therefore, most of the rubber particles that comprise the skin are oriented in the flow direction and little toughening effect is imparted to the transverse direction. The function of the rubber particles is to ensure that large deformations can occur in the matrix without producing a crack that is large enough to cause fracture. In nominal sample [Fig. 2 (b)], the rubber domains are more randomly arranged in all three directions than cracked sample, approximately in random three-dimensional array. This random orientation effectively improves crazing resistance in the rubber-oriented direction and in the transverse direction.

Table I summarized the effect of processing temperature on the tensile properties of ABS/PC alloy resin. The abbreviation of the sample code in Table II, ABS/PC-225, for example, means that the ABS/PC was press molded at 225°C. The tensile strength and elongation at break of dumbbell samples was not changed until 250°C. In contrast ABS/PC-275, an approximately 80% overall decrease in the elongation at break was observed than that of ABS/PC-225. This indicated that ABS/PC resin little affected the tensile properties in processing temperature range.

To analysis the reason of crack phenomenon, Moldflow simulation was conducted using a single cavity mold with direct sprue gating into the part. The dimension of screw and location of sprue gate were shown in Figure 3. The detail processing parameters are summarized in Table II.

Figure 4 shows the filling time and injection pressure results for two injection-molding conditions. The results of filling time analysis show the path of the plastic through the part. The filling time analysis that uses a range of colors indicated that the regions

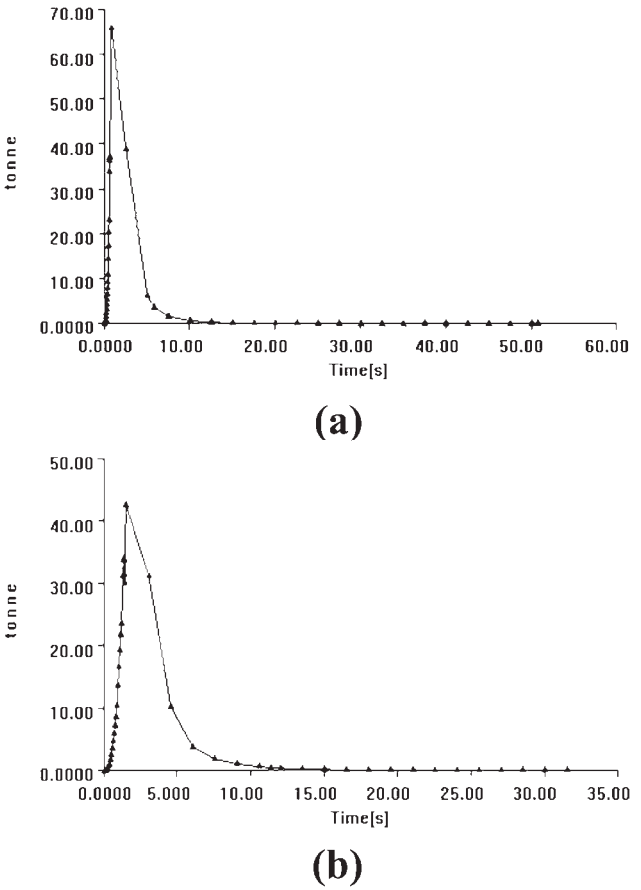

Figure 5 Clamp force changes of the 1st (a) and 2nd (b) condition during injection molding.

first filled through the last region to fill. The results showed that the filling pattern for screw is fairly uniform without any hesitation effect for both condition. The part should be filled in less than 0.64 s for 1st condition [Fig. 4 (a)] and 1.41 s for 2nd condition [Fig. 4 (c)]. Filling time results determine whether all flow paths fill at the same time, balanced flow, hesitation, and overpacking. Injection pressure result displays injection pressure when the selected point was filled. The injection pressure required to fill this part is well within the range of the molding equipment [Fig. 4 (b,d)]. The results can be used to implement other parameter changes to improve filling such as higher or lower injection pressure, moving gate location, and changes to the parts geometry.

Table III demonstrates injection pressure and flow rate changes during filling stage. When applying the first injection molding condition, the maximum injection pressure reaches about 92 MPa at 0.61 s. This seems that the recommended injection pressure for ABS/PC limitation (below 80MPa) will be over approximately 14% exceeded. In Figure 4(d) from 2nd condition, the maximum injection pressure might be estimated about 82.9 MPa at 1.35 s. It is very reasonable value for ABS/PC.

Figure 5 compares the clamp force changes of 1st and 2nd injection molding conditions. The mold is closed within the platen arrangement and clamped using necessary force to hold the mold shut during the plastic injection cycle, thus preventing plastic leakage over the face of the mold. After the required cooling time, the mold is then opened by the clamping motor. In case of 1st condition, the maximum clamp force (65.8 ton) was about 55% higher than that of 2nd condition (42.5 ton). When the clamp force of the machine is exceeded, the molded part was stretched. The mold will open the amount of the stretch increasing the wall thickness of the part. This deformation causes wall thickness variation, which results in both structural and cosmetic defects [Fig. 1 (b)].

Figure 6 show the analysis results of shear rate for 1st and 2nd injection molding simulations. The results can be used to identify areas of high-shear rate through the cavity. When the polymer injected to the mold cavity, polymer melt flows from high-pressure areas to low-pressure areas. Therefore, shear rate is derived from the wall shear stress and the fluidity, which are quantities calculated in the analysis.

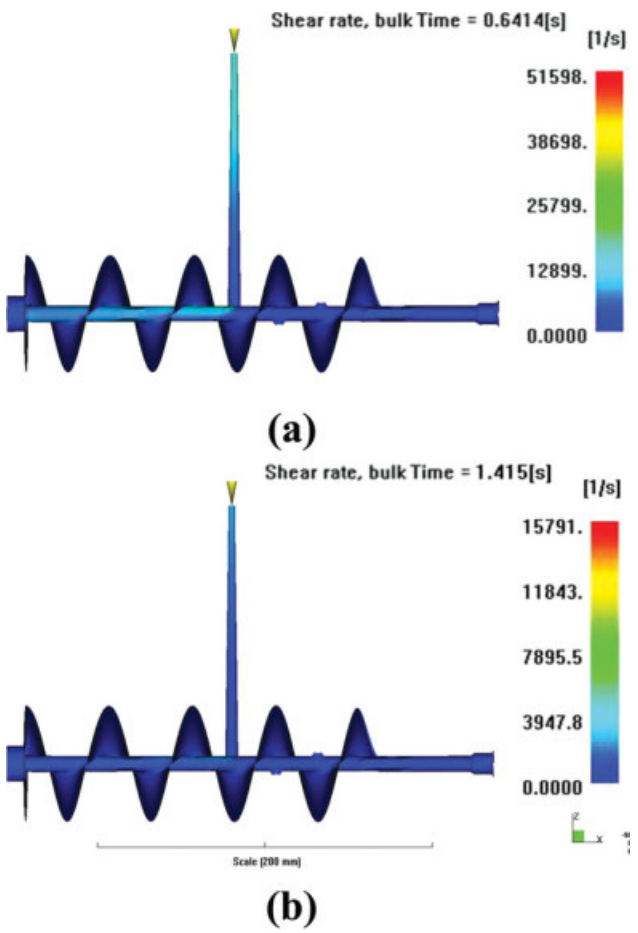

Figure 6 Results of the shear rate analysis for 1st (a) and 2nd (b) injection molding conditions. [Color figure can be viewed in the online issue, which is available at www.interscience.wiley.com.]

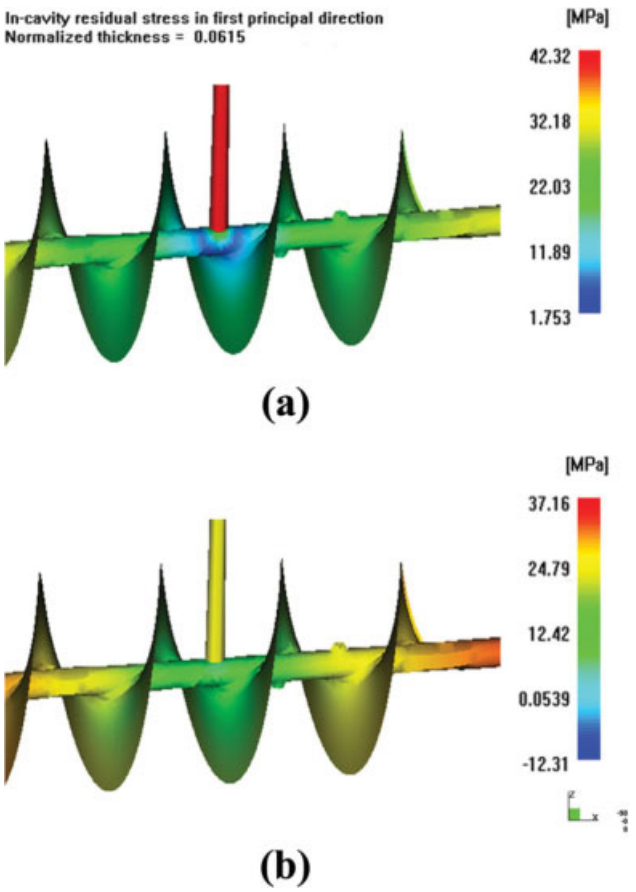

Figure 7 Analysis results of the residual stress for 1st (a) and 2nd (b) conditions. [Color figure can be viewed in the online issue, which is available at www.interscience.wiley.com.]

For 1st condition, the shear rate was experienced by the polymer melt during the injection molding process maximum 51,598 s^{-1}. The recommended shear rate for ABS/PC below 40,000 s^{-1} will be over approximately 29% exceeded. Ideally, the shear rate should be uniform from the injection location to the last point of to fill. Analysis of 2nd condition showed a very uniform shear rate as indicated by the colors showing the part being filled uniformly at very low-shear rate increase differential. The maximum shear rate takes place passing through the sprue gate area [Fig. 6 (a)] and exceeded shear rate originates residual stress for injection molding part (Fig. 7).

CONCLUSIONS

To investigate the reason of crack phenomenon, ABS/PC alloy were injection molded in a screw sample using an actual injection molding condition in factory and the cracked morphology of screw after mechanical stress has been studied by SEM. ABS/PC has a microstructure with the phase separation between components. PC was the continuous phase in alloy resin and ABS was dispersed in the PC matrix. In the micrographs taken on the surface of cracked sample ABS rubber domains tend to align in the direction of mold flow, whereas for nominal sample, the rubber domains are more randomly arranged in all three directions. The tensile properties of the hot-pressed ABS/PC sheets at 225, 250, and 275°C were also investigated. The tensile strength and elongation at break of hot-pressed ABS/PC samples was not changed until 250°C. This indicated that ABS/PC resin little affected the tensile properties in processing temperature range.

As revealed from the Moldflow simulation, high melt flow rate results to an increase of the filling rate of ABS/PC melts into the mold cavity and its injection pressure. This increase the clamp force and leads to higher shear rate resulting to a considerable increase of residual stress. To control this negative effect of increased residual stress on final parts, the reduction of injection rate is considered. This reduces both shear rate of polymer melts and residual stress through the sprue gate. As a result, at higher melt flow condition, the maximum shear rate takes place passing through the sprue gate area and exceeded shear stress remains residual stress in injection-molded part. These results confirmed that higher injection rate can induce the residual stress originated dispersant in ABS/PC orientation through the melt flow becoming losing toughening effect and core shift for final product. This study provides a better understanding of the crack phenomenon for injection-molding screw and gives a better part quality, reduces rework, and scrapping of materials.

References

1. Salari, D.; Ranjbar, H. Iranian Polym J 2008, 17, 599.
2. Arostegui, A.; Sarrionandi, M.; Aurrekoetxea, J.; Urrutibeascoa, I. Polym Degrad Stab 2006, 91, 2768.
3. Rybnicek, J.; Lach, R.; Lapcikova, M.; Steidl, J.; Krulis, Z.; Grellmann, W.; Slouf, M. J Appl Polym Sci 2008, 109, 3210.
4. Boldizar, A.; Moller, K. Polym Degrad Stab 2003, 81, 359.
5. Patel, A. C.; Brahmbhatt, R. B.; Devi, S. J Appl Polym Sci 2003, 88, 72.
6. Sung, Y. T.; Kim, Y. S.; Lee, Y. K.; Kim, W. N.; Lee, H. S.; Sung, J. Y.; Yoon, H. G. Polym Eng Sci 2007, 47, 1671.
7. Huang, J.-C.; Wang, M.-S. Adv Polym Technol 1989, 9, 293.
8. Yan, R. J.; Yang, B. J Appl Polym Sci 1994, 23, 1063.
9. Liu, X.; Bertilsson, H. J Appl Polym Sci 1999, 74, 510.
10. Tademir, M. J Appl Polym Sci 2003, 93, 2521.
11. Sun, S. L.; Tan, Z. Y.; Zhou, C.; Zhang, M.; Zhang, H. X. Polym Compos 2007, 28, 484.
12. Sun, S. L.; Tan, Z. Y.; Xu, X. F.; Zhon, C.; Ao, Y. H.; Zhang, H. X. J Polym Sci Part B Polym Phys 2005, 43, 2179.
13. Chen, L.; Li, J. H.; Zhoub, H. M.; Li, D.; He, Z. C.; Tang, Q. J Mater Process Technol 2008, 208, 90.
14. Parvez, M. A.; Ong, N. S.; Lam, Y. C.; Tor, S. B. J Mater Process Technol 2002, 121, 27.
15. Spiina, R. J Mater Process Technol 2004, 155, 1497.
16. Ozcelik, B.; Sonat, I. Mater Des 2009, 30, 367.
17. Kambour, R. P. J Polym Sci Part A 1964, 2, 4165.
18. Park, E. S. Polym Compos 2008, 29, 1111.
19. Lee, S. S.; Kim, J. Y.; Park, M.; Lim, S. H.; Choe, C. R. J Polym Sci Part B Polym Phys 2001, 39, 2589.